

MammoDL: Mammographic Breast Density Estimation using Federated Learning

Keshava Katti¹, Ramya Muthukrishnan², Angelina Heyler¹, Sarthak Pati^{3,4,5}, Aprupa Alahari², Michael Sanborn¹, Emily F. Conant⁵, Christopher Scott⁶, Stacey Winham⁶, Celine Vachon⁶, Pratik Chaudhari¹, Despina Kontos^{3,5*}, Spyridon Bakas^{3,4,5*}.

Affiliations:

¹Department of Electrical and Systems Engineering, University of Pennsylvania, Philadelphia, PA, USA.

²Department of Computer and Information Science, University of Pennsylvania, Philadelphia, PA, USA.

³Center for Biomedical Image Computing and Analytics (CBICA), University of Pennsylvania, Philadelphia, PA, USA.

⁴Department of Pathology & Laboratory Medicine, Perelman School of Medicine, University of Pennsylvania, Philadelphia, PA, USA.

⁵Department of Radiology, Perelman School of Medicine, University of Pennsylvania, Philadelphia, PA, USA.

⁶Department of Health Sciences Research, Mayo Clinic, Rochester, MN, USA.

*Corresponding authors. Email: despina.kontos@pennmedicine.upenn.edu, sbakas@upenn.edu.

Abstract: Assessing breast cancer risk from imaging remains a subjective process, in which radiologists employ computer aided detection (CAD) systems or qualitative visual assessment to estimate breast percent density (PD). More advanced machine learning (ML) models have become the most promising way to quantify breast cancer risk for early, accurate, and equitable diagnoses, but training such models in medical research is often restricted to small, single-institution data. Since patient demographics and imaging characteristics may vary considerably across imaging sites, models trained on single-institution data tend not to generalize well. In response to this problem, MammoDL is proposed, an open-source software tool that leverages UNet architecture to accurately estimate breast PD and complexity from digital mammography (DM). With the Open Federated Learning (OpenFL) library, this solution enables secure training on datasets across multiple institutions. MammoDL is a leaner, more flexible model than its predecessors, boasting improved generalization due to federation-enabled training on larger, more representative datasets.

One-Sentence Summary: MammoDL uses UNet deep learning architecture to quantitatively assess breast tissue density and complexity from mammograms and enables a data privacy approach by using federated learning.

Keywords: Breast Cancer Risk, Digital Mammography, Breast Density, Deep Learning, Machine Learning, Federated Learning, OpenFL.

1. Introduction

Breast cancer remains the most frequent cancer among women, with about 1 in 8 women in the United States developing breast cancer over the course of her lifetime [1]. Furthermore, breast cancer is the most common cause of cancer-related death for women worldwide [2]. The goal of mammographic screening is to reduce the mortality rate of breast cancer. As such, digital mammography (DM) has become the most standard and reliable method for breast screening today. Randomized trials and incidence-based mortality studies show a notable decrease in breast cancer mortality due to participation in mammography screenings [3-5]. In particular, mammography is highly effective in identifying breast cancers before they become fatal [6]. While mammography may be widely considered as the gold standard of breast screening, it suffers from relatively poor sensitivities ranging from 75% to 85%, with the lowest sensitivity in detecting cancers in women with the densest breast tissue [7]. In the United States, a growing portion of screenings are with digital breast tomosynthesis (DBT), which reconstructs a pseudo-3D image of the breast from several x-ray projections [8], but this technique still suffers from diminished sensitivity as breast density increases. Mammography screenings consist of two-view, mediolateral oblique (MLO) and craniocaudal (CC), bilateral examinations captured as full-field digital mammography (FFDM) images. Radiologists then perform a visual grading of breast density based on the American College of Radiology's Breast Imaging Reporting and Data Systems (BI-RADS). Some radiologists employ simple computer-aided detection (CAD) systems, which generally present limited improvements [9], especially in comparison to their machine learning (ML) counterparts.

Breast density not only limits the sensitivity of mammographic screenings but is also a major risk factor for breast cancer [10]. Over 43% of women in the United States between the age of 40 to 74 have heterogeneously or extremely dense breasts [11]. The most frequent method to grade breast density is subjective, using the BI-RADS classification of breast density based on mammographic images [12-13]. This method does not provide a continuous, real-valued percent density (PD), which would help a radiologist better monitor changes in a patient's breast density that point to heightened breast cancer risk, but rather classifies the breast into one of four density categories.

Current efforts to automate breast density estimates from mammographic images come in the form of commercially available software and research tools. The semi-automated thresholding tool Cumulus remains the current gold-standard area-based breast density estimation method for breast cancer screenings. Commercial software for volumetric breast composition measurement, like Quantra [14] and Volpara [15], show strong association with Cumulus [16] but with several key limitations. These tools determine breast density from x-ray beam interaction models, which make underlying assumptions on metadata to simplify estimates that can lead to inaccurate results [9], especially if some of the prerequisite metadata is not available. Such commercial software may be expensive and may suffer from limited interpretability, as the tools do not output a spatial map delineating the dense tissue from the non-dense tissue in the mammogram. Nonetheless, fully automated volumetric breast density estimation from DBT shows significant promise toward outperforming area-based estimates from DM [17]. Research tools [18-30] come with their own set of limitations. First, with the exception of LIBRA, such tools are not freely available, which not only decreases their likelihood of adoption but also the ability to benchmark their performance with other available PD estimation methods. Second, these research tools have been trained on small, single-institution datasets [10], a consequence of the data silo problem that plagues the medical imaging field.

Upon the advent of deep learning (DL), convolutional neural networks (CNN) have become the workhorse for fully automated mammographic density estimation tools [9]. Such

algorithms rely on sufficiently large and diverse datasets for training, but these datasets can be tremendously difficult to obtain in the medical field. Furthermore, single-institution datasets are not sufficient to provide a representative sample for model training and can lead to low-accuracy generalization [31]. In addition, multi-institutional collaborations that employ centrally shared patient data present numerous privacy and ownership concerns. The solution to these concerns is a novel paradigm for multi-site collaboration called federated learning [31], which allows model training to leverage data across multiple decentralized institutions without sharing data between institutions. Instead, the training process is distributed to each of the data owners and then aggregated into a single model, which not only addresses access rights and privacy concerns from multi-institutional collaborations but vastly increases the generalizability of DL-based medical imaging models as compared to collaborative data sharing (CDS) [31].

This work presents MammoDL, a breast PD estimation tool that builds upon Deep-LIBRA [10], an ML-based improvement to the Laboratory for Individualized Breast Radiodensity Assessment (LIBRA) tool [32]. Deep-LIBRA utilizes two specialized UNet architectures, one for image background removal and the other for identification of the pectoralis muscle. In contrast, MammoDL combines these two steps into one, using a single UNet to perform breast segmentation, including pectoralis muscle removal. Furthermore, while Deep-LIBRA segments the dense tissue by training a support vector machine (SVM) on pixel- and superpixel-level radiomic features, MammoDL trains another UNet to perform this segmentation. Thus, MammoDL is a fully DL-based pipeline for PD estimation that is more lightweight and flexible than Deep-LIBRA. Lastly, MammoDL leverages federated learning capabilities offered by the Open Federated Learning (OpenFL) library [33] to increase the accuracy and generalizability of breast PD estimation with respect to the ground-truth labels produced by a “gold-standard” Cumulus reader. It should be noted that MammoDL is designed to be a hybrid model that combines an ML algorithm with a radiologist assessment, which is shown to be more effective than either of the two operating independently [34].

2. Materials and Methods

MammoDL was conceived as the solution to three different problems facing the broader breast cancer risk assessment community. First, ML-based breast PD estimation tools tended to include numerous segmentation steps or classification/regression tasks, leading to overly complex models that would either generalize poorly or present significant computational costs that limited their usefulness. As a result, the goal was for MammoDL to be a lean ML model with comparable accuracy to its predecessor, Deep-LIBRA. Feature pyramids to detect objects at different scales [35] have already penetrated the medical imaging space, with examples like multi-class segmentation in chest radiographs [36], which motivated MammoDL to execute a multi-segmentation task that offered better generalization to new mammogram images (Fig. 1b). Second, the problem of small, single-institution training datasets was addressed by incorporating a federated learning pipeline into MammoDL, a measure taken to further enhance model generalization (Fig. 1a). Third, it became clear that most breast PD estimation tools were not freely available, which prompted MammoDL to be shared on GitHub for all those interested in the code underlying this work.

2.1. Study Datasets

The dataset used for model training and validation (Table 1) consisted of negative FFDM screening exams obtained from the Hospital of the University of Pennsylvania (HUP), Philadelphia, PA, and the Mayo Clinic (MC), Rochester, MN [10]. It included 3,314 bilateral CC-view images from 1,662 women from the MC and 1,147 bilateral MLO-view images from 115

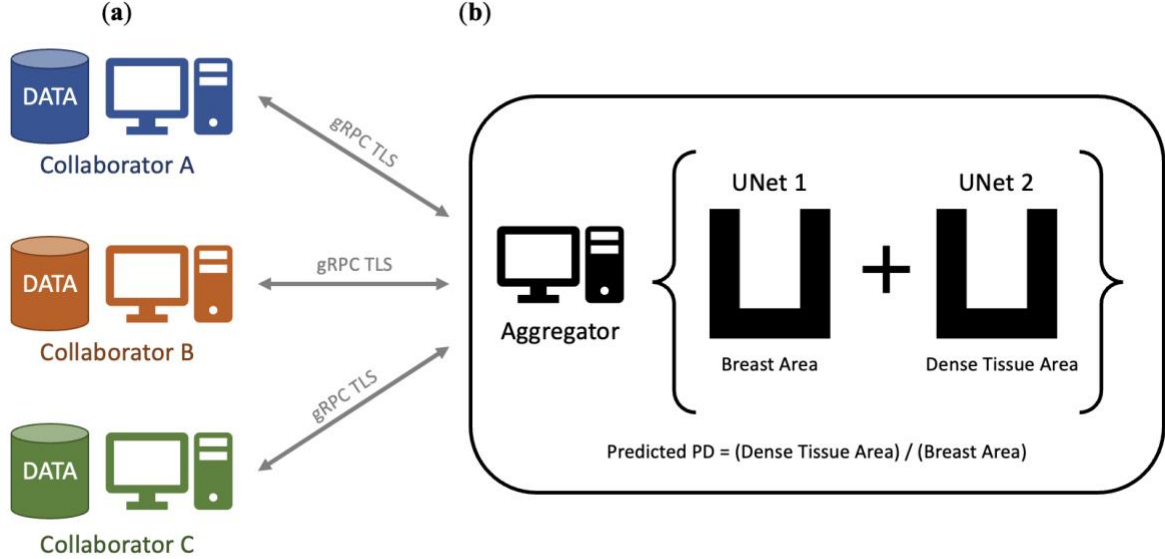


Fig. 1. System-level diagram of MammoDL. (a) Three collaborator nodes are shown, with each performing local training and then transferring the relevant tasks, model and optimizer weights, and other metrics to the aggregator node. (b) The aggregator node represents the two UNet architectures with ResNet34 encodings. Model/metric updates occur in the aggregator node, which train the model to execute segmentation of the breast and dense tissue based on information from all of the collaborators combined. After training is complete, a user can run inference on a new FFDM image to return a breast PD estimation and a spacial mapping that shows the dense tissue delineated from the non-dense tissue.

women from HUP. The ground-truth PD labels were curated on Cumulus by a “gold-standard” (> 20 years of experience estimating PD with Cumulus) human reader. The data from HUP is very racially diverse, which is an important dataset characteristic to accurately assess breast PD [37].

In preparation for the multi-segmentation task, all images were labeled with breast masks such that Class 0 corresponded to the background and pectoralis muscle, while Class 1 corresponded to the breast. What remained was the portion of the mammogram containing only the breast, which acted as the input for the second segmentation model, in which Class 0 corresponded to the non-dense tissue, while Class 1 corresponded to the dense tissue.

Institution	MC	HUP
Number of Images	3,314	1,147
Number of Women	1,662	575
Screening Start Date	2008	2010
Screening End Date	2012	2014
White (%)	98	47
Black (%)	—	53
Other (%)	2	—

Table 1. General characteristics corresponding to the dataset. Each dataset is accompanied by its institution, the number of FFDM images present, the number of women in the screening cohort, the year that the screening began, the year that the screening finished, the percent of white subjects present in the screening, the percent of black subjects present in the screening, and the percent of other racial subjects present in the screening.

2.2. Model Selection and Pre-Processing

Due to the wide use of residual connections in many state-of-the-art neural network architectures and their contributions to breakthroughs in computer vision, the ResNet was selected for this medical imaging task. ResNet architecture not only eases the challenges of training deep neural networks (e.g., by avoiding the vanishing gradient and degradation problems) but boasts outstanding generalization to new data points [38]. The ResNet is employed as the encoder for a UNet, a widely used segmentation module that operates by first down-sampling and then up-sampling an image, creating the “U”-like shape for which it is named. The specific ResNet architecture selected was the ResNet34, and the weights were obtained from pre-training on ImageNet data [39]. Modifying the UNet with a pre-trained ResNet34 encoder (Fig. 2) brings the aforementioned ResNet architecture advantages to the segmentation task plus an increase in the speed of training due to ImageNet pre-training [40]. MammoDL consists of two such modified UNets, the first for identifying the breast from the entire mammogram and the second for delineating the dense tissue region from the breast area.

Pre-processing of the HUP and MC input mammograms (Fig. 3a), which were stored in DICOM format, was executed as follows. To begin, the images were converted into PNG format. Then, a series of pre-processing scripts from Deep-LIBRA were run, which removed the metal tag in the mammogram, adjusted pixel intensities to the range [0, 255], down-sampled the image to 512×512 , and adjusted the contrast to accentuate the dense tissue in the breast. The pre-processed images are then fed through the dual UNet model (Fig. 3b, 3c). The predicted segmentations from each UNet are then resampled to the original image size. The number of pixels in each predicted segmentation are calculated as a measure of area, with the area of the dense tissue region divided by the area of the breast region to return the breast PD (Fig. 3d).

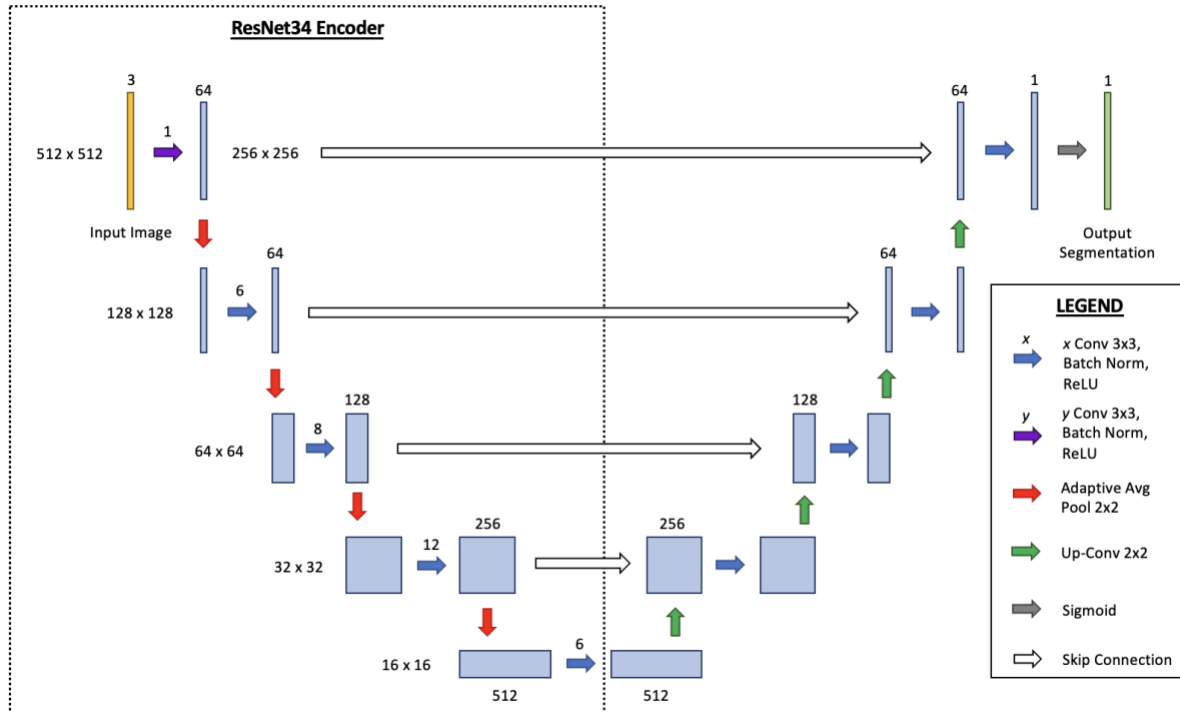


Fig. 2. Diagram of UNet with ResNet34 encoder. The left-hand portion of the UNet architecture corresponds to the “down-sampling” or “encoder” section, where the ResNet34 leverages 2×2 adaptive average pooling to

progressively reduce the dimensions of the mammogram image while increasing the number of feature maps. The ResNet34 operates in five distinct blocks separated by pooling layers, the first corresponding to a single 7×7 convolutional layer with batch normalization and ReLU activation and the last four corresponding to 32 3×3 convolutional layers with batch normalization and ReLU activation. The last layer in the ResNet34 is typically a fully-connected classifier layer, which is omitted in this UNet architecture. The left-hand portion represents the “up-sampling” or “decoding” section, which involves mirror-like 2×2 up-convolution operations separating convolutional layers until the mammogram image returns to its original size, albeit with only a single channel.

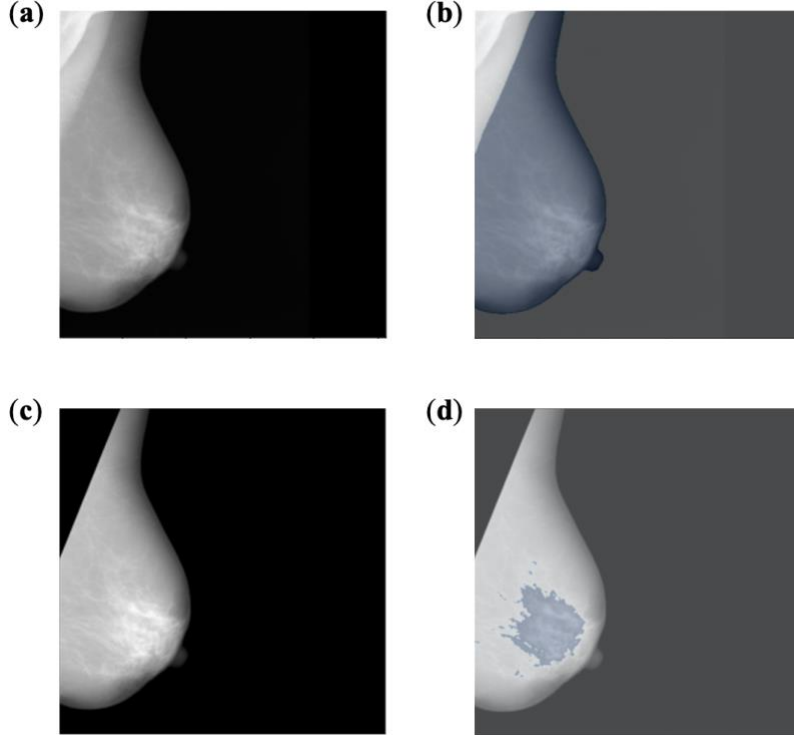


Fig. 3. Stages of the segmentation process in the MammoDL training pipeline. (a) This image shows an unprocessed FFDM in MLO-view from the HUP dataset. (b) After pre-processing, which includes removal of the metal tag, normalization to $[0, 255]$, down-sampling to 512×512 , and adjustment of contrast, the first UNet segments the breast from all other parts of the FFDM image, including the background and pectoralis muscle. Some data augmentation does occur at this stage, limited to flips across the x- and y-axis. (c) The background and pectoralis muscle are removed from the image entirely. Since the initial image was in MLO-view, the absence of the pectoralis muscle is noticeable. The area (i.e., number of pixels) corresponding to the breast is returned. (d) The second UNet delineates the dense tissue from the non-dense tissue. The area corresponding to the dense tissue is returned. The output of the second segmentation task is divided by the output of the first segmentation task, representing the proportion of dense tissue detected in the FFDM image. This value is returned as a percentage.

2.3. Federated Learning

The primary motivation for training the MammoDL model in a federated manner was to expand the size and diversity of the medical training data and facilitate multi-institutional collaborations without having to share the data among institutions. In the field of medical imaging, the impact of federated learning to a ML-based model cannot be understated, with its addition increasing generalization accuracy by up to 35% [41]. In the federated learning framework, each participant is known as either a collaborator or aggregator node. For the purpose of this work, collaborator nodes are hospitals that own a dataset of FFDM images in which the dense breast

tissue is labeled. The DL model is trained locally at each collaborator node. The aggregator node is connected to the collaborator nodes by remote procedure calls (gRPC). OpenFL enables these calls to occur via a mutually authenticated transport layer security (TLS) network connection. Through this secure channel, the collaborator nodes pass tasks, model and optimizer weights, and other metrics in order for the aggregator node to run its own model with the learning information provided by the collaborators.

OpenFL was used to simulate a federated learning scenario, where the MC and HUP were collaborator nodes, while MammoDL was the aggregator node. To avoid cross-institutional data sharing, MammoDL aggregated the model weights across all datasets by taking a weighted average of updates after each epoch, where the weights were proportional to the dataset size. OpenFL ensured that the multi-institutional collaborations were secure, especially for those ML model builders who seek to protect their model intellectual property or those data holders who wish to uphold the privacy of their information [33].

3. Results

The MammoDL model was evaluated by calculating the mean absolute error (MAE) between the true and predicted percent density values across the validation data. MAE was chosen over mean squared error (MSE), or root mean squared error (RMSE) for its interpretability to clinicians, as MAE directly estimates the average error of the model in its percent density prediction. Further, there is a demonstrated need to train on multi-institutional datasets (Table 2), as models trained on both HUP and MC data significantly outperform those trained on either HUP or MC data only. Models trained on solely HUP or MC data tended not to generalize well to new data. The model trained with federated learning achieved nearly the same performance as the centralized model, at last opening the door to secure multi-institutional collaborations (Table 2).

Training Type	Training Data	MAE on MC Data (%)	MAE on HUP Data (%)
Federated	HUP + MC	3.0896	4.2806
Centralized	HUP	5.0671	5.4404
Centralized	MC	5.6265	4.2658
Centralized	HUP + MC	3.7931	3.9741

Table 2. Performance of MammoDL model using federated versus centralized training. As expected, the models trained on both the HUP and MC data perform better than the training on either the HUP data or the MC data in isolation, which provides strong motivation for the need for multi-institutional collaboration in ML-based medical imaging. The performance of the MammoDL model on the centralized and federated training schemes are very close. But the centralized training scheme presents numerous privacy and ownership concerns, which prevents such collaborations from taking place altogether. The federated training scheme emulates the performance of the centralized scheme while maintaining the privacy of patient mammogram data. Therefore, the federated learning pipeline represents a crucial addition to breast PD estimation tools in order to ensure generalization performance is maximized.

The generalization performance of the MammoDL model is compared with that of some breast PD estimation tools mentioned in the introduction of this work (Fig. 4). It is found that MammoDL outperforms both Deep-LIBRA and LIBRA. Even with an optimized cutoff value for risk stratification, Quantra suffers from a sensitivity of 65% and a specificity of 77% when performing BI-RADS classification, where scores of D3/D4 denote high-risk densities and D1/D2 denote low-risk densities [42]. As Volpara requires the same metadata as Quantra, these software tools tend to behave similarly [10], while the outputs of semi-automated thresholding tools, like

Cumulus, are known to vary noticeably based on the expertise of the individual operating the tool [12]. As a result, MammoDL and Deep-LIBRA are the standout performers when it comes to generalization to unseen mammogram images, with both models boasting strong testing accuracy metrics. The crucial difference between MammoDL and Deep-LIBRA is that MammoDL offers a federated learning pipeline that, when trained on more than HUP and MC data, will exhibit even better performance due to learning from larger, more diverse training data. Furthermore, MammoDL is a leaner, more flexible model that requires fewer segmentation steps and no non-DL classifiers.

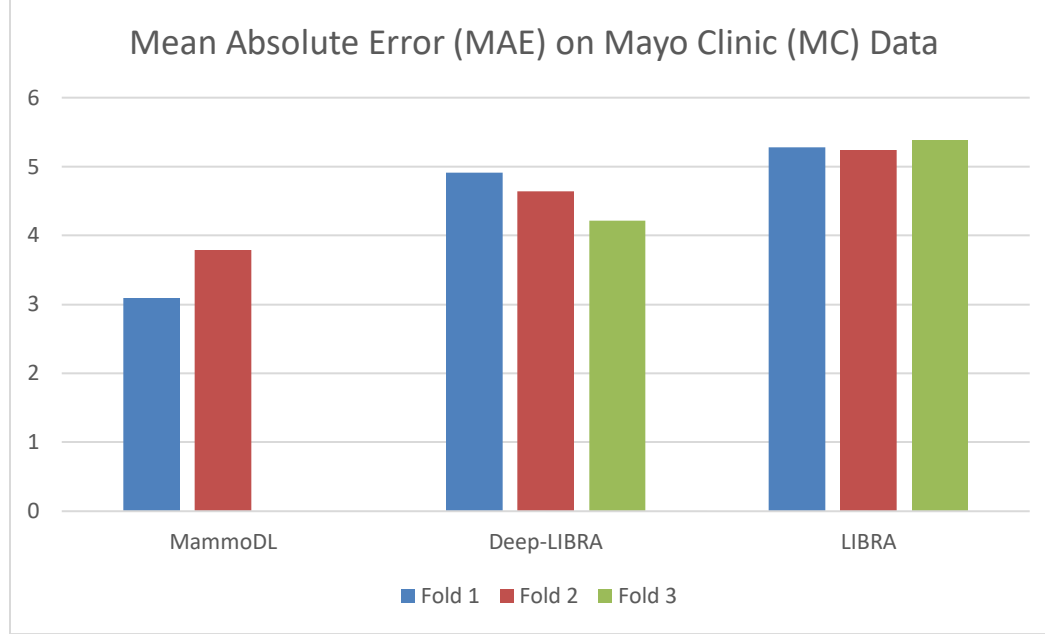


Fig. 4. Generalization performance of MammoDL in comparison to other breast PD estimation tools. This bar plot illustrates the testing accuracy exhibited by MammoDL, Deep-LIBRA, and LIBRA. The y-axis represents the percent error with respect to the the “gold-standard” Cumulus values. Deep-LIBRA has three bars corresponding to the three SVM models resulting from 3-fold cross validation, while LIBRA has three bars corresponding to its percent error on the same held-out folds [10]. MammoDL has a two bars, the former representing the OpenFL-simulated performance of the federated model and the latter showing the results of the centralized model (Table 2). Notice that the generalization behavior of the federated and centralized MammoDL models are better than those of both Deep-LIBRA and LIBRA.

4. Discussion and Conclusion

A deep learning pipeline was implemented to calculate breast PD from input mammograms. The MammoDL model produces a validation MAE of less than 5% and an interpretable spatial map showing the segmented breast and dense tissue regions that clinicians value over black-box predictions. A federated training capability was presented that preserves privacy while maintaining the benefits of training on multi-institutional datasets, enabled by OpenFL. In the future, the goal is to incorporate datasets from more institutions to further validate the robustness of this model and its federated training algorithm across diverse populations, as well as to integrate the training pipeline into a larger framework, such as the Generally Nuanced Deep Learning Framework (GaNDLF) [43], which would allow for wider distribution, more robust

training (by leveraging a standardized set of pre-processing, augmentation, anonymization, and DL architectures), and easier hardware-independent deployment.

MammoDL is currently seeking to bridge this gap by creating a user interface for clinicians to easily use this model for breast cancer risk assessment. This user interface, implemented with React and Node.js, is a hybrid model intended to supplement the expertise of radiologists. Since MammoDL outputs a predicted PD value and a spatial map that identifies the dense tissue from the non-dense tissue, these results are explainable to a radiologist, who can visually determine whether the output of our model aligns with their own assessment. Based on user testing at Penn Medicine, Cumulus can be non-intuitive and difficult to operate, offering far too many outputs to be useful and understandable. The MammoDL user interface outputs a single quantitative measure (PD) to complement other social determinants of health. As such, this model helps standardize current diagnostic work by radiologists, while discouraging overreliance on the algorithm, also known as automation bias. This user interface is still in development and hence is only discussed in the conclusion of this work.

A limitation of this work is its reliance on DM-based breast density to determine breast cancer risk. While automated quantitative assessment of breast density has been shown to be superior to human evaluations [12, 44], such a binary categorization of breast tissue is a simplified model. More specifically, patterns of breast parenchymal complexity, as formed by x-ray attenuation of fatty, fibroglandular, and stromal tissues, are linked with breast cancer risk. Density measures typically reveal the relative amount of fibroglandular tissue in the breast. Such measures are increasingly considered to be limited in their description of the complexity of breast parenchymal patterns [45]. Density-based models that combine traditional risk factors may be more accurate at predicting overall risk of breast cancer than models based only on breast density [9]. Gathering a range of mammographic texture features, including histogram, co-occurrence, run-length, and structural, would help characterize parenchymal complexity and thereafter a corresponding complexity score that elucidates breast cancer risk [45].

With the growing consensus that volumetric breast density estimates from DBT images have stronger connections with breast cancer than area-based or model-approximated volumetric density measures from DM images [17], MammoDL is limited to the amount of information that can be learned from a 2D versus a pseudo-3D image. However, there is strong potential that MammoDL could be repurposed for a transfer learning task. Such a learning framework involves pre-training a deep learning network on a dataset, keeping a large portion of the internal parameters constant, and fine-tuning the parameters of the final layers of the network for a new application [8]. As such, a network trained on DM images, like MammoDL, could feasibly be fine-tuned to predict breast density in DBT images. Such a transfer learning model represents exciting future work toward learning from both DM images, the most standard method for breast screening today, as well as DBT images as they become more ubiquitous.

All of the work described here is freely available for those who would like to iterate and improve upon this model. Please see this GitHub page (<https://github.com/ramyamut/MammoDL>) for access.

References and Notes

1. Howlader N., Noone A.M., Krapcho M., Miller D., Brest A., Yu M., Ruhl J., Tatalovich Z., Mariotto A., Lewis D.R., Chen H.S., Feuer E.J., Cronin K.A. SEER Cancer Statistics Review, 1975-2016, *National Cancer Institute* (2019).

2. Lauby-Secretan, B., Scoccianti, C., Loomis, D., Benbrahim-Tallaa, L., Bouvard, V., Bianchini, F., Straif, K. Breast-Cancer Screening — Viewpoint of the IARC Working Group. *New England Journal of Medicine* **372** (24) (2015).
3. Tabar, L., Vitak, B., Chen, T.H., Yen, A.M., Cohen, A., Tot, T., Chiu, S.Y., Chen, S.L., Fann, J.C., Rosell, J., Fohlin, H., Smith, R.A., Duffy, S.W. Swedish two-county trial: impact of mammographic screening on breast cancer mortality during 3 decades. *Radiology* **260**, 658-663 (2011).
4. IARC Working Group on the Evaluation of Cancer-Preventive Strategies. *Breast Cancer Screening* **15**, IARC Press (2016).
5. Njor, S., Nystrom, L., Moss, S., Paci, E., Broeders, M., Segnan, N., Lynge, E., Euroscreen Working Group. Breast cancer mortality in mammographic screening in Europe: a review of incidence-based mortality studies. *Journal of Medical Screening* **19**, 33-41 (2012).
6. Duffy, S.W., Tabár, L., Yen, A.M.-F., Dean, P.B., Smith, R.A., Jonsson, H., Törnberg, S., Chen, S.L.-S., Chiu, S.Y.-H., Fann, J.C.-Y., Ku, M.M.-S., Wu, W.Y.-Y., Hsu, C.-Y., Chen, Y.-C., Svane, G., Azavedo, E., Grundström, H., Sundén, P., Leifland, K., Frodis, E., Ramos, J., Epstein, B., Åkerlund, A., Sundbom, A., Bordás, P., Wallin, H., Starck, L., Björkgren, A., Carlson, S., Fredriksson, I., Ahlgren, J., Öhman, D., Holmberg, L., Chen, T.H.-H. Mammography screening reduces rates of advanced and fatal breast cancers: Results in 549,091 women. *Cancer* **126**, 2971-2979 (2020).
7. Domingo, L., Hofvind, S., Hubbard, R.A., Roman, M., Benkeser, D., Sala, M., Castells, X. Cross-national comparison of screening mammography accuracy measures in U.S., Norway, and Spain. *European Radiology* **26**, 2520-2528 (2016).
8. Sechopoulos, I., Teuwen, J., Mann, R. Artificial intelligence for breast cancer detection in mammography and digital breast tomosynthesis: State of the art. *Seminars in Cancer Biology* **72**, 214-225 (2021).
9. Bitencourt, A., Naranjo, I.D., Lo Gullo, R., Saccarelli, C.R., Pinker, K. AI-enhanced breast imaging: Where are we and where are we heading? *European Journal of Radiology* **142**, 109882 (2021).
10. Maghsoudi, O.H., Gastounioti, A., Scott, C., Pantalone, L., Wu, F., Cohen, E.A., Winham, S., Conant, E.F., Vachon, C., Kontos, D. Deep-LIBRA: An artificial-intelligence method for robust quantification of breast density with independent validation in breast cancer risk assessment. *Medical Image Analysis* **73**, 102138 (2021).
11. Sprague, B.L., Gangnon, R.E., Burt, V., Trentham-Deitz, A., Hampton, J.M., Wellman, R.D., Kerlikowske, K., Miglioretti, D.L. Prevalence of mammographically dense breasts in the United States. *Journal of the National Cancer Institute* **106** (10) (2014).
12. Sprague, B.L., Conant, E.F., Onega, T., Garcia, M.P., Beaber, E.F., Herschorn, S.D., Lehman, C.D., Tosteson, A.N.A., Lacson, R., Schnall, M.D., Kontos, D., Haas, J.S., Weaver, D.L., Barlow, W.E., PROSPR Consortium. Variation in mammographic breast density assessments among radiologists in clinical practice: a multicenter observational study. *Annals of Internal Medicine* **165** (7), 457-464 (2016).
13. Irshad, A., Leddy, R., Ackerman, S., Cluver, A., Pavic, D., Abid, A., Lewis, M.C. Effects of changes in BI-RADS density assessment guidelines (fourth versus fifth edition) on breast density assessment: intra-and interreader agreements and density distribution. *American Journal of Roentgenology* **207** (6), 1366-1371 (2016).
14. Hartman, K., Highnam, R., Warren, R., Jackson, V. Volumetric Assessment of Breast Tissue composition from FFDM Images. *International Workshop on Digital Mammography* **5116**, 33-39 (2008).

15. Highnam, R., Brady, S.M., Yaffe, M.J., Karssemijer, N., Harvey, J. Robust Breast Composition Measurment. *International Workshop on Digital Mammography* **6136**, 378-385 (2010).
16. Kontos, D. Bakic, P.R., Acciavatti, R.J., Conant, E.F., Maidment, A.D.A. A Comparative Study of Volumetric and Area-Based Breast Density Estimation in Digital Mammography: Results from a Screening Population. *International Workshop on Digital Mammography* **6136**, 378-385 (2010).
17. Gastounioti, A., Pantalone, L., Scott, C.G., Cohen, E.A., Wu, F.F., Winham, S.J., Jensen, M.R., Maidment, A.D.A., Vachon, C.M., Conant, E.F., Kontos, D. Fully Automated Volumetric Breast Density Estimation from Digital Breast Tomosynthesis. *Radiology* **301** (3) (2021).
18. Keller, B.M., Nathan, D.L., Wang, Y., Zheng, Y., Gee, J.C., Conant, E.F., Kontos, D. Estimation of breast percent density in raw and processed full field digital mammography images via adaptive fuzzy c-means clustering and support vector machine segmentation. *Medical Physics* **38** (8), 4903-4917 (2012).
19. Mustra, M., Grgic, M., Rangayyan, R.M. Review of recent advances in segmentation of the breast boundary and the pectoral muscle in mammograms. *Medical & Biological Engineering & Computing* **54**, 1003-1024 (2016).
20. Li, Y., Chen, H., Yang, Y., Yang, N. Pectoral muscle sgmentation in mammograms based on homogenous texture and intensity deviation. *Pattern Recognition* **46** (3), 681-691 (2013).
21. Shi, P., Zhong, J., Rampun, A., Wang, H. A hierarchical pipeline for breast boundary segmentation and calcification detection in mammograms. *Computers in Biology and Medicine* **96**, 178-188 (2018).
22. Anitha, J., Peter, J.D., Pandian, S.I.A. A dual stage adaptive thresholding (DuSAT) for automatic mass detection in mammograms. *Computer Methods and Programs in Biomedicine* **138**, 93-104 (2017).
23. Ferrari, R.J., Rangayyan, R.M., Desautels, J.E.L., Borges, R.A., Frere, A.F. Auto- matic identification of the pectoral muscle in mammograms. *IEEE Transactions on Medical Imaging* **23** (2), 232-245 (2004).
24. Kwok, S.M., Chandrasekhar, R., Attikiouzel, Y., Rickard, M.T. Automatic pectoral muscle segmentation on mediolateral oblique view mammograms. *IEEE Transactions on Medical Imaging* **23** (9), 1129-1140 (2004).
25. Mustra, M., Grgic, M. Robust automatic breast and pectoral muscle segmentation from scanned mammograms. *Signal Processing* **93** (10), 2817-2827 (2013).
26. Nagi, J., Kareem, S.A., Nagi, F., Ahmed, S.K. Automated breast profile segmentation for ROI detection using digital mammograms. *2010 IEEE EMBS Conference on Biomedical Engineering and Sciences (IECBES)*. IEEE, 87-92 (2010).
27. Taghanaki, S.A., Liu, Y., Miles, B., Hamarneh, G. Geometry-based pectoral mus- cle segmentation from MLO mammogram views. *IEEE Transactions on Biomedical Engineering* **64** (11), 2662-2671 (2017).
28. Rampun, A., Morrow, P.J., Scotney, B.W., Winder, J. Fully automated breast boundary and pectoral muscle segmentation in mammograms. *Artificial Intelligence in Medicine* **79**, 28-41 (2017).
29. Czaplicka, K., Włodarczyk, J. Automatic breast-line and pectoral muscle segmentation. *Schedae Informaticae* **20** (2011).
30. Dembrower, K., Liu, Y., Azizpour, H., Eklund, M., Smith, K., Lindholm, P., Strand, F. Comparison of a deep learning risk score and standard mammographic density score for breast cancer risk prediction. *Radiology* **294** (2), 265-272 (2020).

31. Sheller, M.J., Edwards, B., Reina, G.A., Martin, J., Pati, S., Kotrotsou, A., Milchenko, M., Xu, W., Marcus, D., Colen, R.R., Bakas, S. Federated learning in medicine: facilitating multi-institutional collaborations without sharing patient data. *Scientific Reports* **10**, 12598 (2020).
32. Keller, B.M., Chen, J., Daye, D., Conant, E.F., Kontos, D. Preliminary evaluation of the publicly available Laboratory for Breast Radiodensity Assessment (LIBRA) software tool: comparison of fully automated area and volumetric density measures in a case-control study with digital mammography. *Breast Cancer Research* **17** (117) (2015).
33. Reina, G.A., Gruzdev, A., Foley, P., Perepelkina, O., Sharma, M., Davidyuk, I., Trushkin, I., Radionov, M., Mokrov, A., Agapov, D., Martin, J., Edwards, B., Sheller, M.J., Pati, S., Moorthy, P.N., Wang, S., Shah, P., Bakas, S. OpenFL: An open-source framework for Federated Learning. *arXiv* (2021).
34. Rodríguez-Ruiz, A., Krupinski, E., Mordang, J., Schilling, K., Heywang- Kobrunner, S.H., Sechopoulos, I., Mann, R.M. Detection of breast cancer with mammography: effect of an artificial intelligence support system. *Radiology* **290**, 305–314 (2019).
35. Lin, T., Dollar, P., Girshick, R., He, K., Hariharan, B., Belongie, S. Feature Pyramid Networks for Object Detection. *arXiv* (2017).
36. Novikov, A.A., Lenis, D., Major, D., Hladuvka, J., Wimmer, M., Buhler, K. Fully Convolutional Architectures for Multiclass Segmentation in Chest Radiographs. *IEEE Transactions on Medical Imaging* **37** (8), 1865–1876 (2018).
37. McCarthy, A.M., Keller, B.M., Pantalone, L.M., Hsieh, M.-K., Synnestvedt, M., Conant, E.F., Armstrong, K., Kontos, D. Racial differences in quantitative measures of area and volumetric breast density. *Journal of the National Cancer Institute* **108** (10), djw104 (2016).
38. He, F., Liu, T., Tao, D. Why ResNet Works? Residuals Generalize. *IEEE Transactions on Neural Networks and Learning Systems* **31** (12), 5349–5362 (2020).
39. Yakubovskiy, P. Segmentation Models Pytorch. *GitHub repository*, qubvel/segmentation_models.pytorch (2020).
40. Jalali, Y., Fateh, M., Rezvani, M., Abolghasemi, V., Anisi, M.H. ResBCDU-Net: A Deep Learning Framework for Lung CT Image Segmentation. *Sensors (Basel)* **21** (1), 268 (2021).
41. Baid, U., Pati, S., Thakur, S., Edwards, B., Sheller, M., Martin, J., Bakas, S. Federated Tumor Segmentation (FeTS) Initiative: The First Large-Scale Real-World Federation. *Neuro-Oncology* **23** (6), 135–136 (2021).
42. Richard-Davis, G., Whittemore, B., Disher, A., Rice, V.M., Lenin, R.B., Dollins, C., Siegel, E.R., Eswaran, H. Evaluation of Quantra Hologic Volumetric Computerized Breast Density Software in Comparison With Manual Interpretation in a Diverse Population. *Breast Cancer: Basic and Clinical Research* **12** (2018).
43. Pati, S., Thakur, S.P., Bhalerao, M., Thermos, S., Baid, U., Gotkowksi, K., Gonzalez, C., Guley, O., Hamamci, I.E., Er, S., Grenko, C., Edwards, B., Sheller, M., Agraz, J., Baheti, B., Bashyam, V., Sharma, P., Haghghi, B., Gastounioti, A., Bergman, m. Mukhopadhyay, A., Tsaftaris, S.A., Menze, B., Kontos, D., Davatzikos, C., Bakas, S. GaNDLF: A Generally Nuanced Deep Learning Framework for Scalable End-to-End Clinical Workflows in Medical Imaging. *arXiv* (2021).
44. Sartor, H., Lang, K., Rosso, A., Borgquist, S., Zackrisson, S., Timberg, P. Measuring mammographic density: comparing a fully automated volumetric assessment versus European radiologists' qualitative classification. *European Radiology* **26**, 4354–4360 (2016).
45. Kontos, D., Winham, S.J., Oustimov, A., Pantalone, L., Hsieh, M., Gastounioti, A., Whaley, D.H., Hruska, C.B., Kerlikowske, K., Brandt, K., Conant, E.F., Vachon, C.M. Radiomic Phenotypes of Mammographic Parenchymal Complexity: Toward Augmenting Breast Density in Breast Cancer Risk Assessment. *Radiology* **290** (1) (2018).

Acknowledgments: This work was supported in part by the University of Pennsylvania Department of Electrical and Systems Engineering Senior Design Fund.

Author Contributions: *Keshava Katti*: Development of initial training scripts, gathering of encoder architecture results, writing (original draft). *Ramya Muthukrishnan*: Development of final training scripts, preparation of data, gathering of model performance metrics. *Angelina Heyler*: Creation of federated learning pipeline via OpenFL, gathering of federated versus centralized model results. *Sarthak Pati*: Support with OpenFL and GaNDLF, writing (review/editing). *Aprupa Alahari, Michael Sanborn*: Development of user interface for clinical use. *Emily F. Conant*: Radiologist insight, user testing, writing (review/editing). *Christopher Scott, Stacey Winham, Celine Vachon*: Data curation, writing (review/editing). *Pratik Chaudhari*: Advisor for DL model selection. *Spyridon Bakas*: Conceptualization of federated learning components, computation resources, writing (review/editing), supervision, project administration. *Despina Kontos*: Conceptualization of breast PD estimation model, computation resources, writing (review/editing), supervision, project administration.

Competing interests: The authors declare no competing interests.